First-order Bose-Einstein condensation with three-body interacting bosons

Hui Hu [1], Zeng-Qiang Yu,[2,3] Jia Wang [1], and Xia-Ji Liu[1]

[1]*Centre for Quantum Technology Theory, Swinburne University of Technology, Melbourne, Victoria 3122, Australia*
[2]*Institute of Theoretical Physics, Shanxi University, Taiyuan 030006, China*
[3]*State Key Laboratory of Quantum Optics and Quantum Optics Devices, Shanxi University, Taiyuan 030006, China*

Bose-Einstein condensation, observed in either strongly interacting liquid helium or weakly interacting atomic Bose gases, is widely known to be a second-order phase transition. Here we predict a first-order Bose-Einstein condensation in a cloud of harmonically trapped bosons interacting with both attractive two-body interaction and repulsive three-body interaction, characterized respectively by an s-wave scattering length $a < 0$ and a three-body scattering hypervolume $D > 0$. It happens when the harmonic trapping potential is weak, so with increasing temperature the system changes from a low-temperature liquidlike quantum droplet to a normal gas and therefore experiences a first-order liquid-to-gas transition. At large trapping potential, however, the quantum droplet can first turn into a superfluid gas, rendering the condensation transition occurring later from a superfluid gas to a normal gas smooth. We determine a rich phase diagram and show the existence of a tricritical point, where the three phases, i.e., quantum droplet, superfluid gas, and normal gas, meet. We argue that an ensemble of spin-polarized tritium atoms could be a promising candidate to observe the predicted first-order Bose-Einstein condensation, across which the condensate fraction or central condensate density jumps to zero and the surface-mode frequencies diverge.

I. INTRODUCTION

Bose-Einstein condensation (BEC) is a ubiquitous quantum phenomenon that occurs in a wide range of many-body systems, including liquid helium [1], atomic Bose gases [2,3], conventional and high-temperature superconductors [4], and even the hypothetical dark matter axions [5]. All the BEC transitions observed so far are of second order and are described by the model F in the XY universality class with $O(2)$ symmetry [6]. In strongly interacting liquid helium, it is a continuous transition from a normal liquid (He I) to a superfluid liquid (He II) across the λ line [1], while in weakly interacting gaseous Bose systems of ^{87}Rb atoms [2,3], it is a smooth transition from a normal gas to a superfluid gas.

In this work we propose that a first-order BEC transition from a superfluid liquid to a normal gas could occur in weakly interacting atomic Bose gases, when the two-body interaction is tuned to be attractive (i.e., the s-wave scattering length $a < 0$) and the resulting mean-field collapse is arrested by a repulsive three-body interaction characterized by the scattering hypervolume $D > 0$. Our proposal is motivated by the recent experimental realizations of liquidlike quantum droplets [7] in dipolar Bose-Einstein condensates [8–10] or two-component Bose-Bose mixtures with attractive interspecies interactions [11–13], which may experience a liquid-to-gas transition at nonzero temperature. However, a careful examination of the temperature effect [14,15] indicates that the Lee-Huang-Yang (LHY) quantum fluctuation, which is the key ingredient of the droplet formation [16–22], is too fragile to finite temperature. As a result, LHY droplets

are thermally destabilized far below the superfluid transition [14,15]. To overcome such a thermal instability, we resort to earlier cold-atom proposals for quantum droplets based on the three-body repulsive interactions [23–28], which play the same role as LHY quantum fluctuations but are less sensitive to temperature. These proposals have regained considerable interest mostly recently [29,30] owing to the brilliant idea by Tan and Zhu that nontrivial three-body effects can be expressed in terms of a single parameter of the hypervolume D [31,32], which can become positive and significant in realistic van der Waals potential for atoms [30]. Quantum droplets supported by the three-body interactions at zero temperature were then discussed [29,30,33].

Here we address the finite-temperature properties of three-body interacting bosons confined in three-dimensional (3D) harmonic traps, by using the standard Hartree-Fock-Bogoliubov-Popov (HFB-Popov) theory [34–36]. At weak trapping potential, we find two phases, a low-temperature quantum droplet and a high-temperature normal gas, separated by the first-order BEC, while at strong trapping potential another superfluid gas phase emerges and replaces the droplet phase. This leads to the conventional smooth BEC transition between a superfluid gas and a normal gas. An intriguing tricritical point is formed in the phase diagram, at which the quantum droplet, superfluid gas, and normal gas intersect. We explore the scenario of realizing such a tricritical point with ultracold atoms, for example, using a cloud of spin-polarized tritium atoms [25,27].

Incidentally, a similar tricritical point has recently been discussed by Son and co-workers for ultraquantum liquids formed by a hypothetical isotope of helium with nuclear mass

less than 4 amu [37,38]. Our results complement their studies and take advantage of the controllability and simplicity with ultracold atoms [3]. The liquid-to-gas transition and BEC transition have also been considered in the context of strongly interacting matter of α particles [39]. Therefore, it turns out that the first-order BEC transition predicted in our work may find wide applications in diverse fields of physics, ranging from atomic, molecular, and optical physics to condensed matter physics and to high-energy particle physics and nuclear physics.

II. MODEL HAMILTONIAN AND HFB-POPOV THEORY

Three-body interacting bosons of mass M in 3D harmonic traps under consideration can be well described by the model Hamiltonian $\hat{H} = \int d\mathbf{r}\,\mathcal{H}(\mathbf{r})$, with the Hamiltonian density

$$\mathcal{H} = \hat{\psi}^\dagger\left(-\frac{\hbar^2\nabla^2}{2M} + V_T - \mu\right)\hat{\psi} + \frac{g}{2}\hat{\psi}^{\dagger 2}\hat{\psi}^2 + \frac{G}{6}\hat{\psi}^{\dagger 3}\hat{\psi}^3. \tag{1}$$

Here $\hat{\psi}(\mathbf{r})$ and $\hat{\psi}^\dagger(\mathbf{r})$ are the annihilation and creation field operators of bosons, respectively, μ is the chemical potential to be fixed by the total number of atoms N, and $g \equiv 4\pi\hbar^2 a/M < 0$ and $G \equiv \hbar^2 D/M > 0$ are the attractive two-body and repulsive three-body interaction strengths, respectively. The harmonic trapping potential $V_T(\mathbf{r}) \equiv M\omega^2 r^2/2$ is necessary to prevent the atoms from escaping in the gaslike phase or the finite-temperature self-evaporation in the droplet state [15,16].

The model Hamiltonian at nonzero temperature T can be conveniently solved by the HFB-Popov theory [34–36]. We decompose $\hat{\psi}(\mathbf{r}, t) \equiv \Phi(\mathbf{r}) + \tilde{\psi}(\mathbf{r}, t)$ into a condensate wave function $\Phi(\mathbf{r})$ and a field operator $\tilde{\psi}(\mathbf{r}, t)$ for noncondensate atoms. From the equation of motion for $\hat{\psi}(\mathbf{r}, t)$, we deduce, within the Popov approximation as shown in Appendix A, (i) the generalized Gross-Pitaevskii equation (GPE) for the condensate wave function

$$\hat{\mathcal{L}}\Phi(\mathbf{r}) = \mu\Phi(\mathbf{r}), \tag{2}$$

where we have defined the operator

$$\hat{\mathcal{L}} \equiv -\frac{\hbar^2\nabla^2}{2M} + V_T + g(n_c + 2\tilde{n}) + G\left(\frac{n_c^2}{2} + 3n_c\tilde{n} + 3\tilde{n}^2\right)$$

and $n_c(\mathbf{r}) \equiv |\Phi(\mathbf{r})|^2$ and $\tilde{n}(\mathbf{r}) \equiv \langle\tilde{\psi}^\dagger(\mathbf{r})\tilde{\psi}(\mathbf{r})\rangle$ are the condensate and noncondensate densities, respectively, and (ii) the coupled HFB-Popov equations for the ηth quasiparticle wave functions u_η and v_η with energy $E_\eta > 0$,

$$\begin{bmatrix} \hat{\mathcal{L}} - \mu + \hat{\mathcal{M}} & \hat{\mathcal{M}} \\ \hat{\mathcal{M}} & \hat{\mathcal{L}} - \mu + \hat{\mathcal{M}} \end{bmatrix}\begin{bmatrix} u_\eta(\mathbf{r}) \\ v_\eta(\mathbf{r}) \end{bmatrix} = E_\eta\begin{bmatrix} +u_\eta(\mathbf{r}) \\ -v_\eta(\mathbf{r}) \end{bmatrix}, \tag{3}$$

where the operator $\hat{\mathcal{M}} \equiv gn_c + G(n_c^2 + 3n_c\tilde{n})$. Once the quasiparticle wave functions are obtained, the noncondensate density can be calculated according to

$$\tilde{n}(\mathbf{r}) = \tilde{n}_{\rm qd}(\mathbf{r}) + \sum_\eta \frac{|u_\eta(\mathbf{r})|^2 + |v_\eta(\mathbf{r})|^2}{e^{\beta E_\eta} - 1}, \tag{4}$$

where $\tilde{n}_{\rm qd}(\mathbf{r}) = \sum_\eta |v_\eta(\mathbf{r})|^2$ is the depletion to the condensate arising from quantum fluctuations and $\beta \equiv 1/k_B T$. In the ab-

sence of the three-body interaction, i.e., $G = 0$, Eqs. (2) and (3) recover the well-known HFB-Popov theory of a weakly interacting Bose gas [35]. In the normal state ($n_c = 0$ and the total density $n = \tilde{n}$), Eq. (3) instead describes the single-particle motion under a mean-field Hartree-Fock interaction potential $2gn + 3Gn^2$.

The Popov approximation amounts to neglecting the anomalous correlation $\tilde{m}(\mathbf{r}) \equiv \langle\tilde{\psi}(\mathbf{r})\tilde{\psi}(\mathbf{r})\rangle$, which is a higher-order effect beyond mean field [34,36]. It ensures the gapless phonon spectrum in the homogeneous limit [34], where the chemical potential is given by $\mu = g(n_c + 2\tilde{n}) + G(n_c^2/2 + 3n_c\tilde{n} + 3\tilde{n}^2)$ and hence $\hat{\mathcal{L}}_{k=0} = \mu$. However, it is worth noting that, at low temperature, the anomalous correlation is at the same order as the quantum depletion in magnitude. For consistency, therefore, we neglect the quantum depletion in the noncondensate density. This treatment is reasonable, since the quantum depletion is typical about 10%, as shown in Appendix C, and its absence recovers the standard GPE for the condensate wave function [23,24,30,33]. In future studies it would be useful to check the applicability of the Popov approximation used in this work through more advanced Monte Carlo simulations. For a dipolar quantum droplet with a similar condensate depletion, the use of extended GPE without anomalous correlation was recently examined by using the path-integral Monte Carlo technique [40]. There is reasonable agreement between the extended GPEs and Monte Carlo simulations [40]. Therefore, we anticipate similar agreement between the HFB-Popov theory and Monte Carlo calculation for a three-body interacting quantum droplet considered in our work.

We also note that the Popov approximation leads to an artificial first-order superfluid transition with a few percent jump in the condensate density [36]. This drawback has nothing to do with the first-order BEC transition predicted in our work, where the sudden jump in the central condensate density at the transition is almost 100% (see Appendix F).

III. RESULTS AND DISCUSSION

We have iteratively solved Eqs. (2) and (3) in a self-consistent way, with the chemical potential μ determined by the number equation $N = \int d\mathbf{r}[n_c(\mathbf{r}) + \tilde{n}(\mathbf{r})] = N_c + N_{\rm th}$. To ease the numerical workload, it is useful to introduce the rescaled units for length $\bar{\mathbf{r}} \equiv \mathbf{r}/\xi$, density $\bar{n} \equiv n/n_0$, and energy $\bar{E}_\eta \equiv M\xi^2 E_\eta/\hbar^2$, where $\xi = \sqrt{D/6\pi^2 a^2}$ is the length scale and $n_0 = 6\pi|a|/D$ is the equilibrium density of zero-temperature quantum droplets (see Appendix B), so the two interaction strengths now become dimensionless: $gn_0 M\xi^2/\hbar^2 \equiv \bar{g} = -4$ and $Gn_0^2 M\xi^2/\hbar^2 \equiv \bar{G} = 6$. The reduced number of particles is given by $\bar{N} = N/n_0\xi^3$, with $n_0\xi^3 = \sqrt{D/6}/\pi^2 a^2$. Hereafter, we consider a concrete case with $n_0\xi^3 = 1$ and without any confusion we will remove the overbar in the rescaled units.

At zero temperature, the use of the rescaled units leads to a simple GPE $(-\nabla^2/2 + \omega^2 r^2/2 - 4\Phi^2 + 3\Phi^4)\Phi = \mu\Phi$, which has been well understood [23,33]. For instance, without harmonic traps ($\omega = 0$), the GPE allows a self-bound quantum droplet with $\Phi \simeq 1$ and $\mu \simeq -1$ for a large reduced number of particles $N \gg 1$ [24,33]. The droplet state is robust below a characteristic trapping frequency, i.e., $\omega \lesssim \sqrt{2}(4\pi/3N)^{1/3} \simeq$
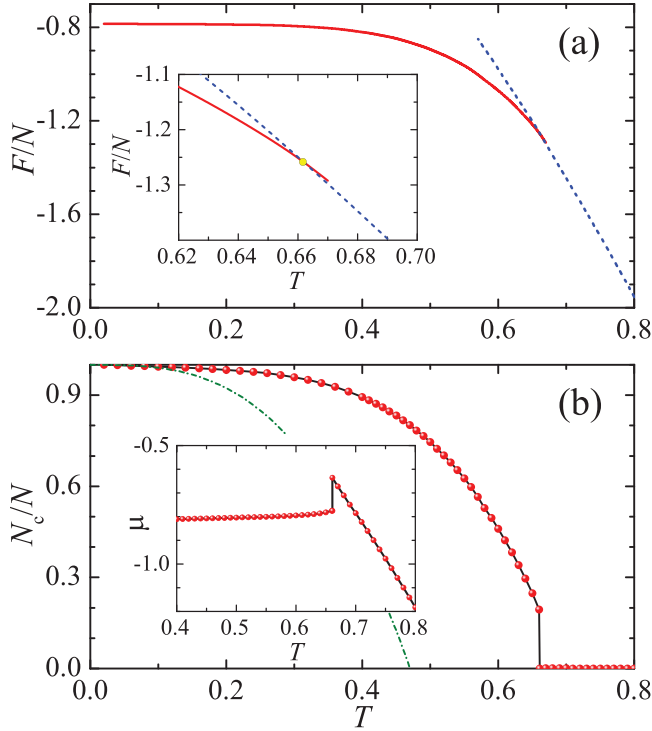
FIG. 1. First-order BEC transition at $N^{1/3}\omega = 0.5$. (a) Temperature dependence of the free energy for the condensed-state solution (red solid line) and for the normal-state solution (blue dashed line). The inset highlights the transition at $T_c \simeq 0.661$. (b) Condensate fraction as a function of temperature. The green dot-dashed line shows $N_c/N = 1 - (T/T_{c0})^3$, where $T_{c0} \simeq 0.9405 N^{1/3}\omega$ is the transition temperature of an ideal Bose gas in harmonic traps [3]. The inset shows a jump in the chemical potential at T_c. The free energy F (or the chemical potential μ) and the temperature T are measured in units of $\hbar^2/M\xi^2$ and $\hbar^2/k_B M\xi^2$, respectively. Here $\xi \equiv \sqrt{D/6\pi^2 a^2}$ is the characteristic length scale of the system.

$2.3N^{-1/3}$ [33]. It is easy to see that if we neglect the finite-size effect for a large number of particles, the properties of the system depend on the product $N^{1/3}\omega$, as in a weakly interacting Bose gas [3]. Most numerical calculations in this work are therefore carried out for $N = 1000$. We also vary N in the range [125,8000] and find no sizable finite-size effect.

A. First-order BEC transition

Let us first consider the finite-temperature thermodynamics at small effective trapping frequency, i.e., $N^{1/3}\omega = 0.5$, as reported in Fig. 1. Remarkably, near the superfluid transition we always find two possible solutions: One comes with a significant condensate fraction, while the other is a completely normal state. To identify which one is the ground-state solution, we calculate the free energy $F = \Omega + \mu N$, where the thermodynamic potential Ω takes the form (see Appendix A)

$$\Omega = \sum_\eta \frac{\ln(1 - e^{-\beta E_\eta})}{\beta} + \int d\mathbf{r}\, \Phi^* \left(-\frac{\hbar^2 \nabla^2}{2M} + V_T - \mu\right)\Phi$$
$$+ \int d\mathbf{r}\left[\frac{g n_c^2}{2} - g\tilde{n}^2 + G\left(\frac{n_c^3}{6} - 3n_c\tilde{n}^2 - 2\tilde{n}^3\right)\right]. \quad (5)$$
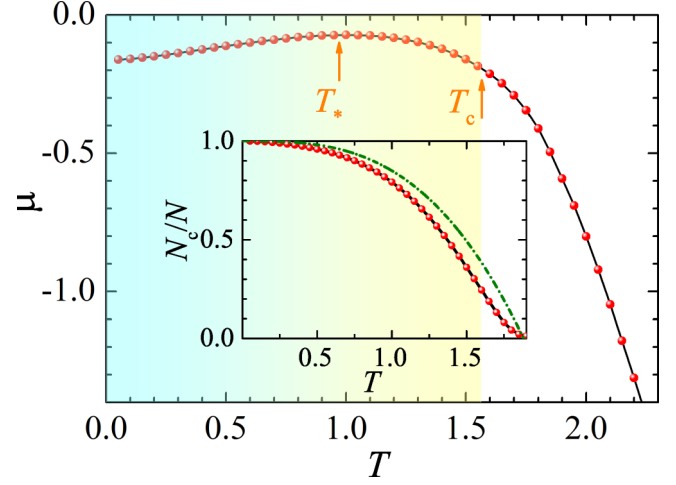

FIG. 2. Second-order BEC transition at $N^{1/3}\omega = 2.0$. The temperature dependence of the chemical potential is smooth and the BEC transition occurs at $T_c \simeq 1.563$. The inset shows the condensate fraction and the green dot-dashed line is the ideal gas prediction $N_c/N = 1 - (T/T_{c0})^3$. The chemical potential μ and the temperature T are measured in units of $\hbar^2/M\xi^2$ and $\hbar^2/k_B M\xi^2$, respectively.

It is readily seen from Fig. 1(a) that the free energies of the two solutions intersect at $T_c \simeq 0.661$ with different slope, clearly indicating a first-order BEC transition. Consequently, the condensate fraction suddenly drops to zero at T_c, as shown in Fig. 1(b). It is also significantly larger than the ideal gas result for noninteracting bosons in harmonic traps, i.e., $N_c/N = 1 - (T/T_{c0})^3$, where $T_{c0} = \omega[N/\zeta(3)]^{1/3}$ with the zeta function $\zeta(3) \simeq 1.202$ [3]. We find that with increasing temperature the noncondensate fraction increases exponentially slowly compared with the usual power-law T^3 behavior in the gaslike phase. This slow increase is due to the discrete excitation spectrum of the self-bound quantum droplet, which persists even in the absence of the trapping potential [33]. We note that the sudden disappearance of the condensate fraction is correlated with a jump in the chemical potential, as plotted in the inset of Fig. 1(b). The observation of a first-order BEC transition at small trapping frequency is the main result of our work.

At large trapping frequency, the situation dramatically changes. A typical case of $N^{1/3}\omega = 2.0$ is presented in Fig. 2. Both the chemical potential and condensate fraction change smoothly when temperature increases, suggesting a second-order superfluid phase transition. We interpret it as a transition from a superfluid gas to a normal gas and therefore use the standard approach to determine a critical temperature $T_c \simeq 1.563$ at which the condensate fraction should change most significantly (i.e., $d^2N_c/dT^2 = 0$) [41]. Our interpretation follows the two observations that the chemical potential is a decreasing function of temperature near the superfluid transition and the condensate fraction lies systematically below the ideal gas prediction (i.e., the green dot-dashed line), both of which are the key features of the second-order transition of a weakly interacting Bose gas [3]. The decreasing condensate fraction is due to the competition between attractive two-body and repulsive three-body interactions. While the attractive two-body interaction tends to increase the condensate fraction
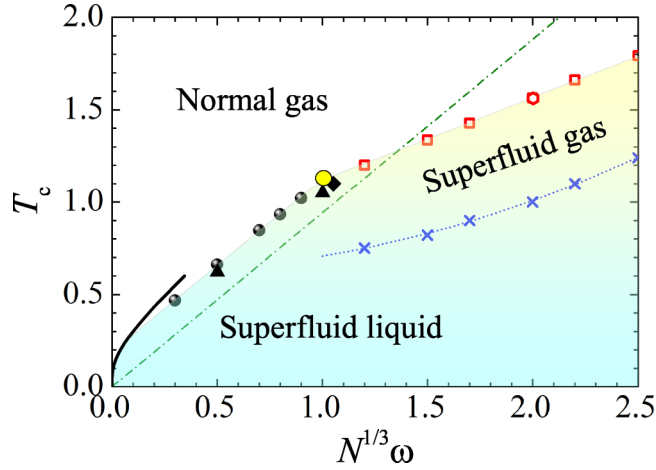
FIG. 3. Critical temperature T_c (closed and open symbols) and crossover temperature T_* (crosses) as a function of $N^{1/3}\omega$. The thick solid line is the critical temperature predicted at small trapping frequency. The green dot-dashed line shows $T_{c0} \simeq 0.9405 N^{1/3}\omega$. The dotted line that connects T_* is a guide for the eye. A tricritical point is highlighted by the yellow circle. Typically, we take $N = 1000$. The change in the reduced number of particles (i.e., the triangles for $N = 125$, diamonds for $N = 3375$, and hexagons for $N = 8000$) does not lead to a sizable difference in T_c. The trapping frequency ω and the critical temperature T_c are measured in units of $\hbar/M\xi^2$ and $\hbar^2/k_B M\xi^2$, respectively.

and also the critical temperature in harmonic traps [3,42], it is overwhelmed by the repulsive three-body interaction. Then, overall, the condensate fraction becomes suppressed. Interestingly, at low temperature the chemical potential is rather an increasing function of temperature up to a turning point (indicated by $T_* \simeq 1.0$ in the figure), which is consistent with the picture of a quantum droplet.[1] Thus, the system seems to cross from a liquidlike droplet over to a gaslike phase at the characteristic temperature T_*.

B. Phase diagram

By calculating the critical temperature T_c and crossover temperature T_* at different effective trapping frequency $N^{1/3}\omega$, we determine a phase diagram in Fig. 3. An intriguing tricritical point appears at $(N^{1/3}\omega)_{\text{tri}} \simeq 1.0$ and $T_{\text{tri}} \simeq 1.13$, where the droplet phase (i.e., superfluid liquid), superfluid gas, and normal gas intersect with others. Below the tricritical trapping frequency, i.e., $N^{1/3}\omega < 1.0$, a superfluid liquid turns into a normal gas via a first-order transition (black closed symbols), while at $N^{1/3}\omega > 1.0$, with increasing temperature, the superfluid liquid first becomes a superfluid gas at the crossover temperature T_* (crosses) and then turns into a normal gas via a smooth second-order phase transition (red open symbols). Note that, with decreasing $N^{1/3}\omega$, the crossover temperature T_* does not converge to the tricritical point. This

is probably due to the difficulty of defining an appropriate crossover temperature in a finite-size system close to the tricritical point (see Appendix E).

At vanishingly small trapping frequency (i.e., $N^{1/3}\omega \to 0$), the critical temperature can be analytically derived, as shown in Appendix D. We find the relation $N^{1/3}\omega = T_c \exp(-1/3T_c)$ and hence $T_c \sim -\ln^{-1}(N\omega^3)$. Due to the logarithmic dependence, T_c could remain sizable at negligible trapping frequency. As the self-evaporation rate of the droplet is very slow at low temperature [43], it seems likely to find a self-bound quantum droplet at small but nonzero critical temperature (i.e., $T_c \simeq 0.1|\mu|$, where the chemical potential $\mu \simeq -1$ sets the energy scale), when we gradually remove the external harmonic trapping potential.

C. Observation of the first-order transition

The predicted first-order BEC transition can be straightforwardly probed from the jump in the condensate fraction, or more readily from the discontinuity in the central condensate density, as we discuss in detail in Appendix F. For small effective trapping frequency, we find that the central condensate density is nearly unchanged below the superfluid transition and suddenly drops to zero right at the critical temperature T_c.

Alternatively, we may probe the first-order transition by measuring the collective excitations of the system. For small trapping frequency, the quantum droplet features peculiar surface modes known as ripplons [16,33,44]. We find that the ripplon mode frequency $\omega_{l\geqslant 2, n=0}$ diverges towards the first-order BEC transition at T_c, as shown in Fig. 4(a). In contrast, at large trapping frequency there seems to be local minimum in the ripplon mode frequencies near the second-order BEC transition, as can be seen from Fig. 4(b). The ripplon mode frequencies also show a characteristic local maximum at about the crossover temperature T_*, which might experimentally be used to locate the smooth crossover from a quantum droplet to a superfluid gas. We emphasize that these two features of local minimum and maximum in the ripplon modes are indicative and their existence should be theoretically examined in a more rigorous manner, by taking into account the co-dynamics of condensate and noncondensate within a random-phase-approximation theory [45]. In this way, the temperature dependence of collective mode frequencies will be determined more accurately and the dipole mode frequency will always be equal to the trapping frequency (i.e., $\omega_{10} = \omega$).

IV. SPIN-POLARIZED TRITIUM ATOMS

In previous theoretical studies of the quantum droplet stabilized by three-body interactions, spin-polarized tritium condensate has been suggested to be a good candidate [25,27]. We have further explored this possibility by investigating the hypervolume D of tritium atoms, inspired by the recent universality work by Mestrom *et al.* [30]. In the absence of Feshbach resonances, the s-wave scattering length $a \simeq -11.92 r_{\text{vdW}}$ and the trimer energy $E_T \simeq -3.50 \times 10^{-3} E_{\text{vdW}}$, where $r_{\text{vdW}} = 6.499 a_0$ and E_{vdW} are the characteristic length and energy of the van der Waals potential of tritium atoms, respectively [25]. The trimer energy differs slightly from the universal value $E_{T,\text{uni}} \simeq -4.45 \times 10^{-3} E_{\text{vdW}}$ [46],

---

[1] The many-body binding energy of a quantum droplet is given by $-\mu$. We may anticipate that the binding energy of the droplet becomes smaller with increasing temperature. Hence, the chemical potential of the droplet increases as temperature increases.
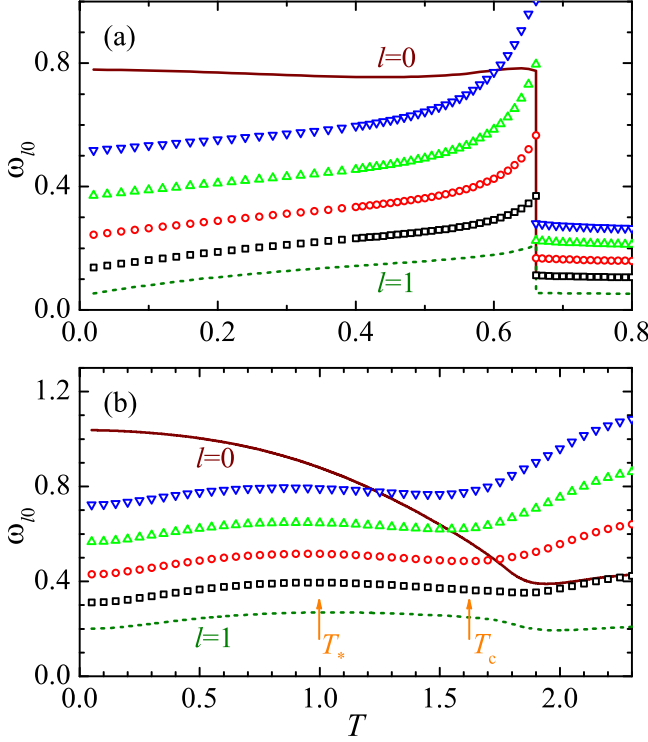
FIG. 4. Mode frequencies $\omega_{l,n=0}$ of the breathing mode ($l = 0$, solid lines), dipole mode ($l = 1$, dotted lines), and surface modes ($l = 2, 3, 4, 5$, symbols from bottom to top) as a function of temperature T at (a) $N^{1/3}\omega = 0.5$ and (b) $N^{1/3}\omega = 2.0$. The dipole mode frequency ω_{10} is not precisely the trapping frequency ω, due to the mean-field interaction potential in the HFB-Popov theory [35]. The mode frequency ω_{l0} (or the trapping frequency ω) and the temperature T are measured in units of $\hbar/M\xi^2$ and $\hbar^2/k_B M\xi^2$, respectively.

suggesting that the universal formalism for the hypervolume $D \simeq 1689R_{\mathrm{hh}}^4$ and $R_{\mathrm{hh}} \sim a$ given by Mestrom *et al.* [30] could be used. As there is no decay dimer channel, D is purely real, without three-body loss [29]. To give some detailed numbers, the scattering length is about $a \simeq -4.1 \times 10^{-9}$ m and the equilibrium density is $n_0 = 6\pi|a|/D \simeq 1.62 \times 10^{23} \mathrm{m}^{-3}$, leading to a gas parameter $n_0|a|^3 \sim 0.01$. We can further apply Feshbach resonances to fine-tune both a and D to realize a cloud of three-body weakly interacting tritium atoms. Cooling and trapping spin-polarized hydrogen and deuterium were recently realized using Zeeman decelerator [47,48]. The same technique can be applied to tritium [49].

V. CONCLUSION

We have proposed that three-body interacting bosons may experience a first-order Bose-Einstein condensation in a weak harmonic trapping potential, in sharp contrast to the conventional smooth condensation transition observed so far. This first-order transition can be unambiguously probed from the sudden jump in the central density and the divergent ripplon mode frequency at the critical temperature. We have suggested that spin-polarized tritium atoms might be a promising candidate for observing the predicted first-order Bose-Einstein condensation transition.

APPENDIX A: THE HFB-POPOV THEORY

We start with the model Hamiltonian for N three-body interacting bosons of mass M in 3D harmonic traps $V_T(\mathbf{r}) \equiv M\omega^2 r^2/2$,

$$\hat{H} = \int d\mathbf{r}\,\mathcal{H}(\mathbf{r}), \tag{A1}$$

where the Hamiltonian density is

$$\mathcal{H} = \hat{\psi}^\dagger\left(-\frac{\hbar^2\nabla^2}{2M} + V_T - \mu\right)\hat{\psi} + \frac{g}{2}\hat{\psi}^{\dagger 2}\hat{\psi}^2 + \frac{G}{6}\hat{\psi}^{\dagger 3}\hat{\psi}^3. \tag{A2}$$

Here $\hat{\psi}(\mathbf{r})$ and $\hat{\psi}^\dagger(\mathbf{r})$ are the annihilation and creation field operators of bosons, respectively, μ is the chemical potential, and the attractive two-body and repulsive three-body interaction strengths are given by

$$g \equiv \frac{4\pi\hbar^2 a}{M} < 0, \tag{A3}$$

$$G \equiv \frac{\hbar^2 D}{M} > 0, \tag{A4}$$

respectively. To derive the HFB-Popov equations, we follow the procedure in the seminal work by Griffin [34] and decompose the field operator $\hat{\psi}(\mathbf{r})$ into a condensate wave function $\Phi(\mathbf{r})$ and a field operator $\tilde{\psi}(\mathbf{r})$ for noncondensate atoms, i.e., $\hat{\psi}(\mathbf{r}, t) \equiv \Phi(\mathbf{r}) + \tilde{\psi}(\mathbf{r}, t)$ and its Hermitian form $\hat{\psi}^\dagger(\mathbf{r}, t) \equiv \Phi^*(\mathbf{r}) + \tilde{\psi}^\dagger(\mathbf{r}, t)$.

In the exact Heisenberg equation of motion for $\hat{\psi}(\mathbf{r})$,

$$i\hbar\frac{\partial\hat{\psi}(\mathbf{r}, t)}{\partial t} = \left(-\frac{\hbar^2\nabla^2}{2M} + V_T - \mu\right)\hat{\psi}(\mathbf{r}, t)$$
$$+ g\hat{\psi}^\dagger\hat{\psi}\hat{\psi}(\mathbf{r}, t) + \frac{G}{2}\hat{\psi}^\dagger\hat{\psi}^\dagger\hat{\psi}\hat{\psi}\hat{\psi}(\mathbf{r}, t), \tag{A5}$$

we take the thermal average and obtain

$$\left(-\frac{\hbar^2\nabla^2}{2M} + V_T - \mu\right)\Phi(\mathbf{r}) + g\langle\hat{\psi}^\dagger\hat{\psi}\hat{\psi}\rangle$$
$$+ \frac{G}{2}\langle\hat{\psi}^\dagger\hat{\psi}^\dagger\hat{\psi}\hat{\psi}\hat{\psi}\rangle = 0. \tag{A6}$$

The last two terms in the equation of motion (A5) can be treated in the self-consistent mean-field approximation [34], namely ($\tilde{n} \equiv \langle\tilde{\psi}^\dagger\tilde{\psi}\rangle$ and $\tilde{m} \equiv \langle\tilde{\psi}\tilde{\psi}\rangle$),

$$\langle\hat{\psi}^\dagger\hat{\psi}\hat{\psi}\rangle = \Phi^2\Phi^* + \Phi^*\langle\tilde{\psi}\tilde{\psi}\rangle + 2\Phi\langle\tilde{\psi}^\dagger\tilde{\psi}\rangle$$
$$= \Phi^2\Phi^* + \Phi^*\tilde{m} + 2\Phi\tilde{n} \tag{A7}$$

and

$$\langle \hat{\psi}^\dagger \hat{\psi}^\dagger \hat{\psi} \hat{\psi} \hat{\psi} \rangle = \Phi^3 \Phi^{*2} + 3\Phi\Phi^{*2}\langle \tilde{\psi}\tilde{\psi} \rangle + 6\Phi^2\Phi^*\langle \tilde{\psi}^\dagger\tilde{\psi} \rangle + \Phi^3\langle \tilde{\psi}^\dagger\tilde{\psi}^\dagger \rangle + 2\Phi^*\langle \tilde{\psi}^\dagger\tilde{\psi}\tilde{\psi}\tilde{\psi} \rangle + 3\Phi\langle \tilde{\psi}^\dagger\tilde{\psi}^\dagger\tilde{\psi}\tilde{\psi} \rangle$$

$$= \Phi^3\Phi^{*2} + 3\Phi\Phi^{*2}\tilde{m} + 6\Phi^2\Phi^*\tilde{n} + \Phi^3\tilde{m}^* + 6\Phi^*\tilde{n}\tilde{m} + 3\Phi(2\tilde{n}^2 + \tilde{m}\tilde{m}^*). \tag{A8}$$

Here we have decoupled the four-field-operator terms according to the Wick theorem,

$$\langle \tilde{\psi}^\dagger\tilde{\psi}\tilde{\psi}\tilde{\psi} \rangle = 3\tilde{n}\tilde{m}, \tag{A9}$$

$$\langle \tilde{\psi}^\dagger\tilde{\psi}^\dagger\tilde{\psi}\tilde{\psi} \rangle = 2\tilde{n}^2 + \tilde{m}\tilde{m}^*. \tag{A10}$$

Therefore, we find the time-independent generalized GPE $[n_c \equiv |\Phi(\mathbf{r})|^2]$

$$\left(-\frac{\hbar^2\nabla^2}{2M} + V_T - \mu\right)\Phi + g(n_c + 2\tilde{n})\Phi + g\tilde{m}\Phi^* + \frac{G}{2}(n_c^2 + 6n_c\tilde{n} + 6\tilde{n}^2 + \Phi^2\tilde{m}^* + 3\tilde{m}\tilde{m}^*)\Phi + \frac{3G}{2}(n_c\tilde{m} + 2\tilde{n}\tilde{m})\Phi^* = 0. \tag{A11}$$

It is well known that a nonzero anomalous correlation $\tilde{m} \equiv \langle \tilde{\psi}\tilde{\psi} \rangle$ gives rise to a gapped excitation spectrum [34,36], even in the absence of the three-body interacting term, which is unphysical. Therefore, we take the Popov approximation $\tilde{m} = 0$ and $\tilde{m}^* = 0$ everywhere in the generalized GPE. This leads to the form

$$\hat{\mathcal{L}}\Phi(\mathbf{r}) \equiv \left[-\frac{\hbar^2\nabla^2}{2M} + V_T + g(n_c + 2\tilde{n}) + G\left(\frac{n_c^2}{2} + 3n_c\tilde{n} + 3\tilde{n}^2\right)\right]\Phi(\mathbf{r}) = \mu\Phi(\mathbf{r}). \tag{A12}$$

The generalized Hartree-Fock-Bogoliubov equation for quasiparticles may be derived from the equation of motion for the field operator $\tilde{\psi}(\mathbf{r})$ of noncondensate atoms [34], which can be obtained by subtracting Eq. (A6) from Eq. (A5). It can also be equivalently derived by expanding the model Hamiltonian to the quadratic terms of $\tilde{\psi}^\dagger$ and $\tilde{\psi}$ [34]. This alternative derivation is useful to determine the expressions of the thermodynamic potential and free energy. Therefore, let us describe it in detail. We first consider the two-body interaction term

$$\hat{\psi}^{\dagger 2}\hat{\psi}^2 = \Phi^2\Phi^{*2} + \Phi^2\tilde{\psi}^\dagger\tilde{\psi}^\dagger + 4\Phi\Phi^*\tilde{\psi}^\dagger\tilde{\psi} + \Phi^{*2}\tilde{\psi}\tilde{\psi} + \tilde{\psi}^\dagger\tilde{\psi}^\dagger\tilde{\psi}\tilde{\psi},$$

$$= [(\Phi^2 + \tilde{m})\tilde{\psi}^\dagger\tilde{\psi}^\dagger + \text{H.c.}] + 4(n_c + \tilde{n})\tilde{\psi}^\dagger\tilde{\psi} + n_c^2 - (2\tilde{n}^2 + \tilde{m}\tilde{m}^*). \tag{A13}$$

In the second line of this equation, we have taken the self-consistent mean-field approximation to $\tilde{\psi}^\dagger\tilde{\psi}^\dagger\tilde{\psi}\tilde{\psi}$, i.e.,

$$\tilde{\psi}^\dagger\tilde{\psi}^\dagger\tilde{\psi}\tilde{\psi} = \tilde{m}\tilde{\psi}^\dagger\tilde{\psi}^\dagger + 4\tilde{n}\tilde{\psi}^\dagger\tilde{\psi} + \tilde{m}^*\tilde{\psi}\tilde{\psi} - (2\tilde{n}^2 + \tilde{m}\tilde{m}^*). \tag{A14}$$

The three-body interaction term can be treated in a similar way. We find that

$$\hat{\psi}^{\dagger 3}\hat{\psi}^3 = n_c^3 + (3\Phi^3\Phi^*\tilde{\psi}^\dagger\tilde{\psi}^\dagger + \text{H.c.}) + 9n_c^2\tilde{\psi}^\dagger\tilde{\psi} + 9n_c\tilde{\psi}^\dagger\tilde{\psi}^\dagger\tilde{\psi}\tilde{\psi} + (3\Phi^2\tilde{\psi}^\dagger\tilde{\psi}^\dagger\tilde{\psi}^\dagger\tilde{\psi} + \text{H.c.}) + \tilde{\psi}^{\dagger 3}\tilde{\psi}^3. \tag{A15}$$

By inserting the mean-field decoupling, i.e.,

$$\tilde{\psi}^\dagger\tilde{\psi}^\dagger\tilde{\psi}^\dagger\tilde{\psi} = 3\tilde{n}\tilde{\psi}^\dagger\tilde{\psi}^\dagger + 3\tilde{m}^*\tilde{\psi}^\dagger\tilde{\psi} - 3\tilde{n}\tilde{m}^*, \tag{A16}$$

$$\tilde{\psi}^{\dagger 3}\tilde{\psi}^3 = 9[\tilde{n}\tilde{m}\tilde{\psi}^\dagger\tilde{\psi}^\dagger + (2\tilde{n}^2 + \tilde{m}\tilde{m}^*)\tilde{\psi}^\dagger\tilde{\psi} + \tilde{n}\tilde{m}^*\tilde{\psi}\tilde{\psi}] - (12\tilde{n}^3 + 18\tilde{n}\tilde{m}\tilde{m}^*), \tag{A17}$$

we obtain that

$$\hat{\psi}^{\dagger 3}\hat{\psi}^3 = [(3\Phi^3\Phi^* + 9n_c\tilde{m} + 9\Phi^2\tilde{n} + 9\tilde{n}\tilde{m})\tilde{\psi}^\dagger\tilde{\psi}^\dagger + \text{H.c.}] + 9(n_c^2 + \Phi^2\tilde{m}^* + \Phi^{*2}\tilde{m} + 4n_c\tilde{n} + 2\tilde{n}^2 + \tilde{m}\tilde{m}^*)\tilde{\psi}^\dagger\tilde{\psi}$$

$$+ n_c^3 - [(9\Phi^2\tilde{n}\tilde{m}^* + \text{H.c.}) + 9n_c(2\tilde{n}^2 + \tilde{m}\tilde{m}^*) + 12\tilde{n}^3 + 18\tilde{n}\tilde{m}\tilde{m}^*]. \tag{A18}$$

By collecting all the bilinear terms in the field operators, we may rewrite the Hamiltonian density within the Hartree-Fock-Bogoliubov approximation as

$$\mathcal{H}_{\text{HFB}} = \frac{1}{2}[\tilde{\psi}^\dagger, \quad \tilde{\psi}]\begin{bmatrix} \hat{\mathcal{K}}_{\text{HFB}} - \mu & \hat{\mathcal{M}}_{\text{HFB}} \\ \hat{\mathcal{M}}_{\text{HFB}} & \hat{\mathcal{K}}_{\text{HFB}} - \mu \end{bmatrix}\begin{bmatrix} \tilde{\psi} \\ \tilde{\psi}^\dagger \end{bmatrix} + \Omega_{\text{HFB}}^{(0)}(\mathbf{r}), \tag{A19}$$

where we have defined the operators

$$\hat{\mathcal{K}}_{\text{HFB}} \equiv -\frac{\hbar^2\nabla^2}{2M} + V_T + 2g(n_c + \tilde{n}) + \frac{3}{2}G(n_c^2 + \Phi^2\tilde{m}^* + \Phi^{*2}\tilde{m} + 4n_c\tilde{n} + 2\tilde{n}^2 + \tilde{m}\tilde{m}^*), \tag{A20}$$

$$\hat{\mathcal{M}}_{\text{HFB}} \equiv g(\Phi^2 + \tilde{m}) + G(n_c\Phi^2 + 3n_c\tilde{m} + 3\Phi^2\tilde{n} + 3n\tilde{m}) \tag{A21}$$

and

$$\Omega_{\text{HFB}}^{(0)}(\mathbf{r}) \equiv \Phi^*\left(-\frac{\hbar^2\nabla^2}{2M} + V_T - \mu\right)\Phi + \frac{g}{2}(n_c^2 - 2\tilde{n}^2 - \tilde{m}\tilde{m}^*) + \frac{G}{6}[n_c^3 - (9\Phi^2\tilde{n}\tilde{m}^* + \text{H.c.})$$

$$- 9n_c(2\tilde{n}^2 + \tilde{m}\tilde{m}^*) - 12\tilde{n}^3 - 18\tilde{n}\tilde{m}\tilde{m}^*] \tag{A22}$$

is the density of the mean-field thermodynamic potential at zero temperature. Let us now take the Popov approximation and set $\tilde{m} = 0$ and $\tilde{m}^* = 0$ in $\hat{\mathcal{K}}_{\text{HFB}}$, $\hat{\mathcal{M}}_{\text{HFB}}$, and $\Omega_{\text{HFB}}^{(0)}(\mathbf{r})$. By further assuming a real ground-state condensate wave function $\Phi(\mathbf{r})$, it is easy to see that $\hat{\mathcal{M}}_{\text{HFB}}$ becomes

$$\hat{\mathcal{M}} = g n_c + G(n_c^2 + 3 n_c \tilde{n}) \qquad (A23)$$

and $\hat{\mathcal{K}}_{\text{HFB}}$ can be rewrite as

$$\hat{\mathcal{K}} = \hat{\mathcal{L}} + \hat{\mathcal{M}}, \qquad (A24)$$

where the operator $\hat{\mathcal{L}}$ is defined in Eq. (A12). Also, $\Omega_{\text{HFB}}^{(0)}(\mathbf{r})$ takes the form

$$\Omega^{(0)}(\mathbf{r}) = \Phi^* \left(-\frac{\hbar^2 \nabla^2}{2M} + V_T - \mu \right) \Phi + g \left(\frac{n_c^2}{2} - \tilde{n}^2 \right)$$
$$+ G \left(\frac{n_c^3}{6} - 3 n_c \tilde{n}^2 - 2 \tilde{n}^3 \right). \qquad (A25)$$

From the Hamiltonian density for the field operators of non-condensate atoms [Eq. (A19)], we directly write down the coupled HFB-Popov equations for the ηth quasiparticle wave functions u_η and v_η with energy $E_\eta > 0$,

$$\begin{bmatrix} \hat{\mathcal{L}} - \mu + \hat{\mathcal{M}} & \hat{\mathcal{M}} \\ \hat{\mathcal{M}} & \hat{\mathcal{L}} - \mu + \hat{\mathcal{M}} \end{bmatrix} \begin{bmatrix} u_\eta(\mathbf{r}) \\ v_\eta(\mathbf{r}) \end{bmatrix} = E_\eta \begin{bmatrix} +u_\eta(\mathbf{r}) \\ -v_\eta(\mathbf{r}) \end{bmatrix}. \qquad (A26)$$

The total thermodynamic potential at finite temperature T is given by

$$\Omega = \Omega_{\text{LHY}}^{(0)} + k_B T \sum_\eta \ln(1 - e^{-\beta E_\eta}) + \int d\mathbf{r} \, \Omega^{(0)}(\mathbf{r}), \qquad (A27)$$

where $\beta = 1/k_B T$ is the inverse temperature and

$$\Omega_{\text{LHY}}^{(0)} \equiv -\sum_\eta \int d\mathbf{r} \, E_\eta |v_\eta(\mathbf{r})|^2 \qquad (A28)$$

is the contribution of quantum fluctuations to the thermodynamic potential, the so-called Lee-Huang-Yang energy term [3]. Once the quasiparticle wave functions are obtained, the noncondensate density can be calculated according to

$$\tilde{n}(\mathbf{r}) = \tilde{n}_{\text{qd}}(\mathbf{r}) + \sum_\eta \frac{|u_\eta(\mathbf{r})|^2 + |v_\eta(\mathbf{r})|^2}{e^{\beta E_\eta} - 1}, \qquad (A29)$$

where $\tilde{n}_{\text{qd}}(\mathbf{r}) = \sum_\eta |v_\eta(\mathbf{r})|^2$ is the depletion to the condensate arising from quantum fluctuations and is the only contribution to density at zero temperature.

Equations (A12) and (A26), together with Eq. (A29) and $n_c = |\Phi(\mathbf{r})|^2$, form a closed set of HFB-Popov equations that should be solved self-consistently [35]. The chemical potential μ should be adjusted to satisfy the number equation $N = \int d\mathbf{r}[n_c(\mathbf{r}) + \tilde{n}(\mathbf{r})] \equiv N_c + N_{\text{th}}$.

The HFB-Popov theory has been extensively used to describe weakly interacting Bose gases at finite temperature [35]. The advantages and shortages of such a theory are now well understood. In particular, it is known that the theory does not provide accurate descriptions at both zero temperature

and temperatures sufficiently close to the superfluid transition [36]. At zero temperature, this is because the anomalous correlation $\tilde{m}(\mathbf{r})$ neglected in the Popov approximation becomes comparable to the normal correlation, i.e., $\tilde{n}_{\text{qd}}(\mathbf{r})$, if we critically examine the role of zero-temperature quantum fluctuations. For the consistency of the theory, it thus seems necessary to discard the quantum depletion $\tilde{n}_{\text{qd}}(\mathbf{r})$ and the LHY energy term $\Omega_{\text{LHY}}^{(0)}$. This treatment is well justified for a weakly interacting Bose gas with a repulsive two-body interaction alone, where the quantum depletion (or the LHY energy) contributes only a few percent to the total density (or the total energy) [35]. For a three-body interacting quantum droplet considered in this work, as we will discuss below, we find that the quantum depletion is typically at about 10%, much smaller than that of a superfluid helium droplet, where 90% of atoms are out of the condensate at $T = 0$. In the vicinity of the superfluid transition T_c, it is also known that the Popov approximation predicts a spurious first-order superfluid transition for a homogeneous Bose gas, as characterized by a very small jump (i.e., about a few percent) in the condensate density [36]. This spurious feature is not important and does not show up when the system is confined in a harmonic trap.

APPENDIX B: NUMERICAL CALCULATIONS

At zero temperature, where the noncondensate density $\tilde{n} = 0$ as we neglect the quantum depletion, the generalized GPE (A12) in free space (i.e., $V_T = 0$) takes the form

$$\left(-\frac{\hbar^2 \nabla^2}{2M} + g|\Phi|^2 + \frac{G}{2}|\Phi|^4 \right) \Phi = \mu \Phi. \qquad (B1)$$

As $g < 0$ and $G > 0$, this GPE admits a self-bound droplet as the ground state for a sufficiently large number of atoms $N = \int d\mathbf{r} |\Phi|^2 \gg 1$. To see this, let us check the case of an infinitely large number of atoms, where we can safely neglect the surface effect and remove the first kinetic term (i.e., the ∇^2 term). We find that the bulk chemical potential ($n = |\Phi|^2$)

$$\mu(n) = gn + \frac{G}{2} n^2 \qquad (B2)$$

and consequently the energy per particle

$$\frac{\epsilon(n)}{n} = \frac{g}{2} n + \frac{G}{6} n^2. \qquad (B3)$$

It is clear that the energy per particle acquires a minimum at the equilibrium density

$$n_0 = \frac{3}{2} \frac{(-g)}{G} = 6\pi \frac{|a|}{D}, \qquad (B4)$$

at which the pressure P vanishes due to the thermodynamic relation

$$P = \left(n^2 \frac{\partial(\epsilon/n)}{\partial n} \right)_{n=n_0} = 0. \qquad (B5)$$

The system is therefore self-bound into a droplet state at zero pressure, in equilibrium with the surrounding vacuum. In the absence of the external harmonic trap, the center density would be fixed to n_0, if we neglect the boundary (surface) effect. When we add the particles to the droplet, the droplet

expands and increases its radius while keeping its bulk density unchanged.

1. Rescaled units

In numerical calculations, it is convenient to introduce the units for length, density, and also energy and to make the equations dimensionless. For the density unit, the equilibrium density n_0 is a natural choice. To fix the length unit ξ, let us require that the three-body term in the energy per particle assumes the simple form

$$\frac{G}{6}n^2 \rightarrow \frac{\bar{G}}{6}\bar{n}^2 = \bar{n}^2, \tag{B6}$$

after we use the rescaled units (as indicated by the bar above the variables). This means that the dimensionless three-body interaction strength is

$$\bar{G} \equiv \frac{Gn_0^2}{\hbar^2/M\xi^2} = 6, \tag{B7}$$

where $\hbar^2/M\xi^2$ is the energy unit related to the length unit ξ. By substituting $G = \hbar^2 D/M$ and the equilibrium density n_0, we find that

$$\xi = \sqrt{\frac{D}{6\pi^2 a^2}}. \tag{B8}$$

It is straightforward to check that the two-body interaction strength then becomes

$$\bar{g} \equiv \frac{gn_0}{\hbar^2/M\xi^2} = -4. \tag{B9}$$

From now on we will use the rescaled units for length $\bar{\mathbf{r}} \equiv \mathbf{r}/\xi$, density $\bar{n} \equiv n/n_0$, energy $\bar{E}_\eta \equiv M\xi^2 E_\eta/\hbar^2$, and trapping frequency $\bar{\omega} = M\xi^2\omega/\hbar$. The rescaled condensate wave function is $\bar{\Phi} = \Phi/\sqrt{n_0}$. The reduced number of particles is given by $\bar{N} = N/n_0\xi^3$, with

$$n_0\xi^3 = \frac{\sqrt{D/6}}{\pi^2 a^2}, \tag{B10}$$

and the number equation becomes

$$\bar{N} = \int d\bar{\mathbf{r}} \frac{n_c(\bar{\mathbf{r}}) + \tilde{n}(\bar{\mathbf{r}})}{n_0} \equiv \bar{N}_c + \bar{N}_{\text{th}}. \tag{B11}$$

Hereafter, for convenience, we consider the specific case with $n_0\xi^3 = 1$. Then we will remove the bar for all the rescaled units. Our choice is motivated by the van der Waals universality for the hypervolume $D \simeq 1689a^4$ in the weakly interacting regime, as recently predicted in Ref. [30]. Therefore, the dimensionless parameter

$$n_0\xi^3 \simeq \frac{\sqrt{1689/6}}{\pi^2} \simeq 1.7, \tag{B12}$$

close to the value that we choose.

In the dimensionless form ($g = -4$ and $G = 6$, and effectively $\hbar = M = 1$), the zero-temperature GPE (B1) then becomes very simple,

$$\left(-\frac{\nabla^2}{2} + \frac{\omega^2 r^2}{2} - 4\Phi^2 + 3\Phi^4\right)\Phi = \mu\Phi, \tag{B13}$$

where we have reinserted the harmonic trap term. We see that this equation depends on two controlling variables, the dimensionless trapping frequency ω and the reduced number of particle N, both of which involve the microscopic parameters of the model Hamiltonian such as the two-body scattering length a and the three-body scattering hypervolume D. Equation (B13) has been discussed in detail in the previous work [33]. It turns out that for a large reduced number of particles, we can neglect the finite-size effect and the properties of the system actually depend on a single parameter $N^{1/3}\omega$. In our calculations, we typically take the reduced number of particles $N = 1000$.

2. Technical difficulties

The dimensionless HPB-Popov equations with the operators $\hat{\mathcal{L}}$ and $\hat{\mathcal{M}}$, obtained by setting $\hbar = M = 1$, $g = -4$, and $G = 6$, can be solved by the routines outlined in previous work [15,33,35]. The following three challenges in the numerical calculations are worth noting.

First, for a droplet state, there are numerous quasiparticle energy levels accumulated just above the particle emission threshold $|\mu|$ [33]. The energy level separation is set by the harmonic trapping frequency ω. To solve this difficulty, we consider a dimensionless trapping frequency $\omega \geqslant 0.03$ and typically use several hundred expansion basis functions in solving the quasiparticle wave functions u_η and v_η for a given angular momentum l (which is a good quantum number for our spherical harmonic traps). Further improvement on the numerical accuracy could be achieved by considering the fifth-order B-spline basis [15]. The B-spline basis would allow us to use an uneven grid, which might better represent the solution wave function. It also allows a higher-order approximation of the derivative operator that appears in the kinetic energy term.

On the other hand, at finite temperature $T \neq 0$ we must iterate the solutions of the GPE (A12) for the condensate wave function and the HFB-Popov equations (A26) for the quasiparticle wave functions, in order to gradually improve the thermal density $\tilde{n}(\mathbf{r})$ for convergence. This iterative procedure turns out to be very slow with increasing temperature. In particular, sufficiently close to the superfluid transition, the small number of condensed particles $N_c \sim O(1)$ implies that the chemical potential μ appearing in the GPE (i.e., the lowest eigenvalue of the operator $\hat{\mathcal{L}}$ in the zero momentum $l = 0$ sector) can no longer be treated as the chemical potential of the whole system. To solve this problem, we introduce a new chemical potential μ_t of the whole system, by requiring that

$$\frac{1}{e^{(\mu-\mu_t)/k_B T} - 1} = N_c. \tag{B14}$$

The difference between the two chemical potentials

$$\mu - \mu_t = k_B T \ln\left(1 + \frac{1}{N_c}\right) \sim \frac{k_B T}{N_c} \tag{B15}$$

is negligibly small away from the superfluid transition when $N_c \gg 1$. However, in the vicinity of the superfluid transition, in the Bose-Einstein distribution function $f_B(E_\eta)$ we have to measure the energy E_η of the Bogoliubov quasiparticles with respect to μ_t, instead of μ. This leads to a modified expression

for the thermal density (in the case of excluding the quantum depletion),

$$\tilde{n}(\mathbf{r}) = \sum_\eta \frac{|u_\eta(\mathbf{r})|^2 + |v_\eta(\mathbf{r})|^2}{e^{\beta(E_\eta + \mu - \mu_t)} - 1}$$

$$= \sum_\eta \frac{|u_\eta(\mathbf{r})|^2 + |v_\eta(\mathbf{r})|^2}{(1 + 1/N_c)e^{\beta E_\eta} - 1}. \quad \text{(B16)}$$

The thermal contribution to the thermodynamic potential in Eq. (A27) is modified in a similar way (i.e., by replacing E_η with $E_\eta + \mu - \mu_t$).

Finally, a high temperature leads to the significant population of the high-energy quasiparticle energy levels, which would require a large number of expansion basis functions in solving the HFB-Popov equations and therefore considerably slow down our numerical calculations. To avoid this problem, we consider the use of the local-density approximation (LDA) for the high-lying quasiparticle wave functions [50]. For this purpose, we introduce a high-energy cutoff E_c. For the quasiparticle energy $E_\eta > E_c$, we treat the quasiparticle wave functions locally (at the position r) as plane waves with amplitudes $u_\mathbf{k}(r)$ and $v_\mathbf{k}(r)$ at the momentum $\mathbf{k}$ [50]. The HFB-Popov equations for the quasiparticles then become

$$\begin{bmatrix} \frac{k^2}{2} + \mathcal{V}_{\text{eff}}(r) & \mathcal{M}(r) \\ \mathcal{M}(r) & \frac{k^2}{2} + \mathcal{V}_{\text{eff}}(r) \end{bmatrix} \begin{bmatrix} u_\mathbf{k} \\ v_\mathbf{k} \end{bmatrix} = E_\mathbf{k} \begin{bmatrix} +u_\mathbf{k} \\ -v_\mathbf{k} \end{bmatrix}, \quad \text{(B17)}$$

where

$$\mathcal{V}_{\text{eff}} = \frac{\omega^2 r^2}{2} - \mu - 8(n_c + \tilde{n}) + 9n_c^2 + 36n_c\tilde{n} + 6\tilde{n}^2, \quad \text{(B18)}$$

$$\mathcal{M} = -4n_c + 6n_c^2 + 18n_c\tilde{n}, \quad \text{(B19)}$$

from which we obtain

$$u_\mathbf{k}^2(r) = \frac{1}{2}\left[\frac{k^2/2 + \mathcal{V}_{\text{eff}}(r)}{E_\mathbf{k}(r)} + 1\right], \quad \text{(B20)}$$

$$v_\mathbf{k}^2(r) = \frac{1}{2}\left[\frac{k^2/2 + \mathcal{V}_{\text{eff}}(r)}{E_\mathbf{k}(r)} - 1\right], \quad \text{(B21)}$$

and

$$E_\mathbf{k}(r) = \sqrt{[k^2/2 + \mathcal{V}_{\text{eff}}(r)]^2 - \mathcal{M}^2(r)}. \quad \text{(B22)}$$

At the position r, therefore the LDA contribution from the continuous high-lying energy levels to the thermal density [i.e., $E_\mathbf{k}(r) > E_c$] is

$$\tilde{n}_H(\mathbf{r}) = \int \frac{d\mathbf{k}}{(2\pi)^3} \frac{[\frac{k^2}{2} + \mathcal{V}_{\text{eff}}(r)]/E_\mathbf{k}(r)}{(1 + 1/N_c)e^{\beta E_\mathbf{k}(r)} - 1}. \quad \text{(B23)}$$

Together with the contribution from the discrete low-lying energy levels

$$\tilde{n}_L(\mathbf{r}) = \sum_{E_\eta < E_c} \frac{|u_\eta(\mathbf{r})|^2 + |v_\eta(\mathbf{r})|^2}{(1 + 1/N_c)e^{\beta E_\eta} - 1}, \quad \text{(B24)}$$

we obtain the total thermal density

$$\tilde{n}(\mathbf{r}) = \tilde{n}_L(\mathbf{r}) + \tilde{n}_H(\mathbf{r}). \quad \text{(B25)}$$

The LDA treatment for the high-lying quasiparticle energy levels turns out to be very efficient. Our numerical results are
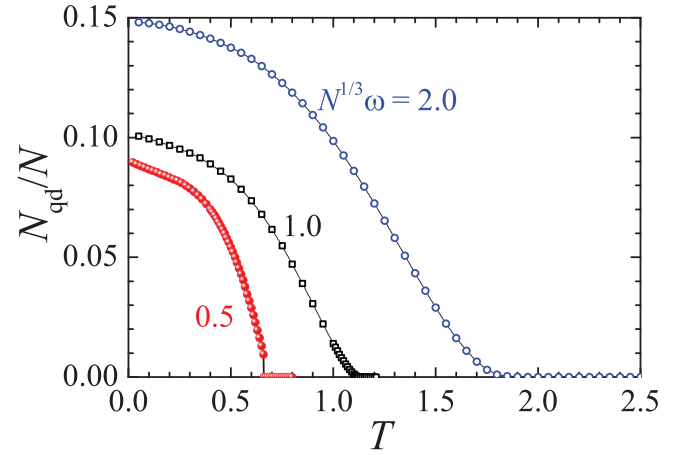

FIG. 5. Quantum depletion N_{qd}/N as a function of temperature at three effective trapping frequencies $N^{1/3}\omega = 0.5$, 1.0, and 2.0. The depletion is typically about 10%. It vanishes when we increase the temperature towards the superfluid transition. The trapping frequency ω and temperature T are measured in units of $\hbar/M\xi^2$ and $\hbar^2/k_B M\xi^2$, respectively.

essentially independent of the cutoff energy E_c, provided it is reasonably large.

APPENDIX C: QUANTUM DEPLETION

We have self-consistently (and iteratively) solved the coupled HFB-Popov equations, without the inclusion of the quantum depletion $\tilde{n}_{\text{qd}}(\mathbf{r})$ in the thermal density $\tilde{n}(\mathbf{r})$. We then calculated the number of quantum depleted atoms $N_{\text{qd}} = \int d\mathbf{r} \sum_\eta |v_\eta(\mathbf{r})|^2$ for a self-consistent check. The results are shown in Fig. 5, where we consider the temperature dependence of the ratio N_{qd}/N at three effective trapping frequencies. We have also tried the inclusion of $\tilde{n}_{\text{qd}}(\mathbf{r})$ in the thermal density $\tilde{n}(\mathbf{r})$ in our numerical iterations and found qualitatively similar predictions.

It is readily seen that the quantum depletion is typically at around 10% at zero temperature. Actually, we would anticipate that the zero-temperature quantum depletion should be a universal function of $n_0\xi^3$ in the absence of the external harmonic trap (i.e., about a few percent at our choice of $n_0\xi^3 = 1$), where the bulk density of the droplet state is precisely the equilibrium density n_0. The increase of the zero-temperature quantum depletion with increasing effective trapping frequency should be contributed to the enhanced central density due to the external trapping potential.

In more detail, without harmonic traps we may estimate the quantum depletion at zero temperature within the standard Bogoliubov theory under the local-density approximation

$$N_{\text{qd}} = \int \frac{d\mathbf{r}\, d\mathbf{k}}{(2\pi)^3} \frac{1}{2}\left(\frac{\frac{\hbar^2 k^2}{2m} + gn_c + Gn_c^2}{\sqrt{\frac{\hbar^2 k^2}{2m}\left(\frac{\hbar^2 k^2}{2m} + 2gn_c + 2Gn_c^2\right)}} - 1 \right), \quad \text{(C1)}$$

where the condensate density $n_c(\mathbf{r}) \simeq n_0 = -3g/2G$ within the self-bound droplet (i.e., $|\mathbf{r}| < R$). By rewriting the

equation into the dimensionless units, we find that ($x = k\xi$)

$$N_{qd} \simeq \frac{4\pi R^3}{3\xi^3} \int_0^\infty \frac{dx}{4\pi^2} x^2 \left(\frac{x^2 + 4}{x\sqrt{x^2 + 8}} - 1 \right) = \frac{2\sqrt{2}}{3\pi^2} \frac{4\pi R^3}{3\xi^3}. \tag{C2}$$

By dividing the total number of atoms $N = \bar{N}(n_0 \xi^3) = (4\pi/3)(R^3/\xi^3)(n_0 \xi^3)$, we obtain

$$\frac{N_{qd}}{N} = \frac{2\sqrt{2}}{3\pi^2} \frac{1}{n_0 \xi^3}, \tag{C3}$$

which is about 9.6% at $n_0 \xi^3 = 1$, in agreement with what we observe in Fig. 5.

At nonzero temperature, as shown in Fig. 5 the quantum depletion decreases as anticipated. It becomes negligibly small close to the superfluid transition. As in this work we are mostly interested in the region near the superfluid transition, the consistent exclusion of the quantum depletion in our HFB-Popov calculations therefore seems well justified.

APPENDIX D: FIRST-ORDER BEC TRANSITION TEMPERATURE

The first-order BEC transition temperature at small effective trapping frequency $N^{1/3}\omega \to 0$ might be analytically derived. To see this, let us consider the free energy $F_S(T)$ of the superfluid quantum droplet state and the free energy $F_N(T)$ of a normal Bose gas.

1. Normal-state free energy $F_N(T)$

For the normal phase, since the trapping frequency is very small, the atomic cloud is dilute and can be treated as a noninteracting Bose gas. The free energy can then be obtained in the semiclassical approximation [3]

$$F_N = \iint \frac{d\mathbf{k} d\mathbf{r}}{(2\pi)^3} \ln(1 - e^{-\beta(\hbar^2 k^2/2m + V_T - \mu)}) + \mu N, \tag{D1}$$

where the chemical potential μ satisfies

$$N = \iint \frac{d\mathbf{k} d\mathbf{r}}{(2\pi)^3} \frac{1}{e^{\beta(\hbar^2 k^2/2m + V_T - \mu)} - 1}. \tag{D2}$$

These Bose-type integrals can be worked out explicitly, with the help of the polylogarithmic function $\mathrm{Li}_\nu(z)$, i.e.,

$$\int_0^\infty d\epsilon \frac{\epsilon^{\nu-1}}{e^{\beta(\epsilon - \mu) - 1}} = (k_B T)^\nu \Gamma(\nu) \mathrm{Li}_\nu(z), \tag{D3}$$

where the fugacity $z \equiv e^{\beta\mu}$ and $\Gamma(\nu)$ is the Gamma function. We find that [3]

$$\frac{F_N}{N} = k_B T \frac{\mathrm{Li}_4(z)}{\mathrm{Li}_3(z)} + \mu, \tag{D4}$$

$$N = \left(\frac{k_B T}{\hbar \omega} \right)^3 \mathrm{Li}_3(z). \tag{D5}$$

In the normal phase, the fugacity z turns out to be very small. Indeed, below the condensation transition the chemical potential μ must turn into the bulk chemical potential of the droplet state, i.e., $\mu_0 = gn_0 + Gn_0^2/2 < 0$, which serves as the energy unit after we rescale and make the equations dimensionless. For example, by taking $g = -4$, $G = 6$, and $n_0 = 1$, we obtain

$\mu_0 = -1$. Therefore, it is reasonable to Taylor expand the expressions of the free energy and the number of particles, in terms of the small fugacity $z \sim e^{\mu_0/k_B T} \ll 1$ at low temperature $k_B T \ll |\mu_0|$. In the rescaled units, after we take $k_B = 1$ and $\hbar = 1$, we then obtain that

$$\frac{F_N}{N|\mu_0|} \simeq T \left(1 - \frac{z}{16} \right) + T \ln z, \tag{D6}$$

$$N\omega^3 \simeq T^3 z \left(1 + \frac{z}{8} \right). \tag{D7}$$

By reexpressing the fugacity z in terms of the temperature T, to the leading order we finally arrive at

$$\frac{F_N}{N|\mu_0|} \simeq 3T \ln \frac{N^{1/3}\omega}{T}. \tag{D8}$$

2. Droplet-state free energy $F_S(T)$

At low temperature, the free energy $F_S(T)$ is essentially the zero-temperature total energy $E(T = 0)$ of the droplet, if we neglect the small surface effect for a large droplet (with $N \gg 1$). By using Eq. (B3), in the rescaled units we find that

$$\frac{F_S}{N|\mu_0|} \simeq -1. \tag{D9}$$

This expression is easy to understand. At zero temperature we anticipate that all the atoms are bounded into the droplet with the binding energy $|\mu_0|$.

3. First-order superfluid transition temperature

Using the condition $F_N(T) = F_S(T)$ at the transition temperature T_c, we obtain

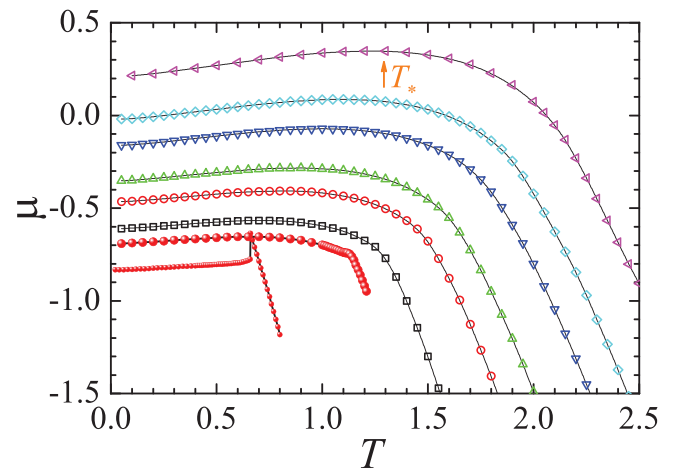$$3T_c \ln \frac{N^{1/3}\omega}{T_c} = -1 \tag{D10}$$

FIG. 6. Temperature dependence of the chemical potential at different effective trapping frequency $N^{1/3}\omega$. From bottom to top, the value of $N^{1/3}\omega$ is 0.5, 1.0, 1.2, 1.5, 1.7, 2.0, 2.2, and 2.5. The chemical potential μ and temperature T are measured in units of $\hbar^2/M\xi^2$ and $\hbar^2/k_B M\xi^2$, respectively.
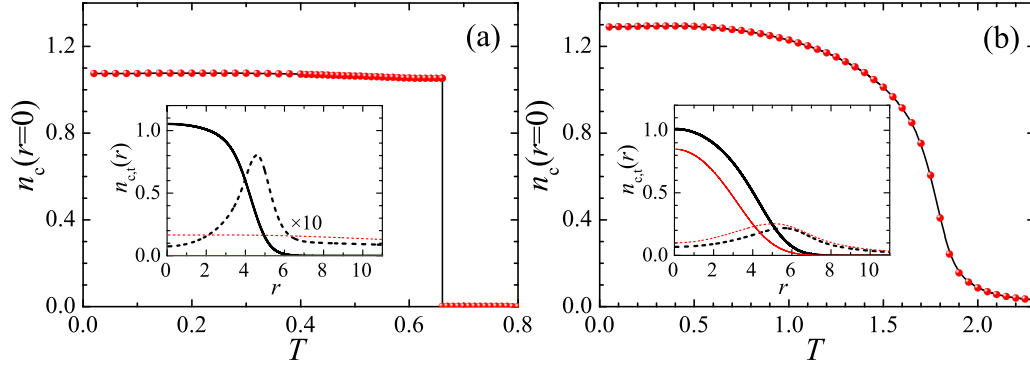
FIG. 7. Temperature dependence of the central condensate density at (a) $N^{1/3}\omega = 0.5$ and (b) $N^{1/3}\omega = 2.0$. The insets show the condensate and thermal density distributions at $T = 0.95T_c$ (black thick curves) and at $T = 1.05T_c$ (red thin curves), respectively. The condensate distribution is plotted as a solid line and the thermal distribution as a dashed line. The trapping frequency ω and temperature T are measured in units of $\hbar/M\xi^2$ and $\hbar^2/k_B M\xi^2$, respectively. Moreover, the radius r is measured in units of ξ and the density is measured in units of the equilibrium density n_0.

or

$$N^{1/3}\omega = T_c \exp\left(-\frac{1}{3T_c}\right). \qquad (\text{D11})$$

By restoring the full units, we find that

$$N^{1/3}\hbar\omega = k_B T_c \exp\left(\frac{\mu_0}{3k_B T_c}\right), \qquad (\text{D12})$$

where the bulk chemical potential takes the form

$$\mu_0 = -\frac{3g^2}{8G}. \qquad (\text{D13})$$

It is clear that the critical temperature eventually goes to zero $T_c \to 0$, when we gradually remove the external harmonic trapping potential $\omega \to 0$.

APPENDIX E: CHARACTERISTIC TEMPERATURE T_* FROM THE CHEMICAL POTENTIAL

At large effective trapping frequency $N^{1/3}\omega > 1.0$, with decreasing temperature the cloud of three-body interacting bosons experiences a conventional smooth second-order phase transition from a normal gas to a superfluid gas at T_c. If we further decrease the temperature below T_c, the system may become a superfluid liquid (i.e., a quantum droplet) at a characteristic temperature T_*, where the chemical potential acquires a maximum in its temperature dependence.

This is not always true, when we decrease the effective trapping frequency to the regime $N^{1/3}\omega < 1.0$, as reported in Fig. 6. In that regime, the temperature dependence of the chemical potential becomes rather flattened. Moreover,

at even smaller effective trapping frequency (i.e., the lowest curve with $N^{1/3}\omega = 0.5$), the chemical potential monotonically increases with increasing temperature, before the sudden (first-order) jump to the chemical potential of a normal phase. We cannot observe that the characteristic temperature T_* smoothly merges with the transition temperature T_c at the tricritical point $(N^{1/3}\omega, T_c)_{\text{tri}} \simeq (1.0, 1.13)$.

APPENDIX F: CENTRAL CONDENSATE DENSITY ACROSS THE SUPERFLUID TRANSITION

The difference in the first-order and second-order BEC transitions can be most easily identified by measuring the central condensate density at the trap center. In Fig. 7 we report the central condensate density as a function of temperature at two different effective trapping frequencies $N^{1/3}\omega = 0.5$ [Fig. 7(a)] and $N^{1/3}\omega = 2.0$ [Fig. 7(b)], at which the system experiences the first-order transition and second-order transition, respectively. The two insets show the spatial distributions of the condensate density and the thermal density before and after the BEC transition (see, for example, the black thick curves at $T = 0.95T_c$ and the red thin curves at $T = 1.05T_c$).

The first-order BEC transition is clearly revealed in the inset of Fig. 7(a), where the central condensate density suddenly jumps to zero while the thermal density (enlarged by ten times in the inset) becomes nearly flat in the region plotted. In sharp contrast, at the second-order BEC transition the central condensate density gradually vanishes as the temperature increases. As illustrated in the inset of Fig. 7(b), there is still a considerable condensate density at $T = 1.05T_c$, due to the finite number of particles (i.e., the finite-size effect).

[1] A. Griffin, *Excitations in a Bose-Condensed Liquid* (Cambridge University Press, Cambridge, 1993).

[2] M. H. Anderson, J. R. Ensher, M. R. Matthews, C. E. Wieman, and E. A. Cornell, Observation of Bose-Einstein condensation in a dilute atomic vapor, Science **269**, 198 (1995).

[3] F. Dalfovo, S. Giorgini, L. P. Pitaevskii, and S. Stringari, Theory of Bose-Einstein condensation in trapped gases, Rev. Mod. Phys. **71**, 463 (1999).

[4] P. A. Lee, N. Nagaosa, and X.-G. Wen, Doping a Mott insulator: Physics of high-temperature superconductivity, Rev. Mod. Phys. **78**, 17 (2006).

[5] P. Sikivie and Q. Yang, Bose-Einstein Condensation of Dark Matter Axions, Phys. Rev. Lett. **103**, 111301 (2009).

[6] P. C. Hohenberg and B. I. Halperin, Theory of dynamic critical phenomena, Rev. Mod. Phys. **49**, 435 (1977).

[7] For a recent review see, for example, F. Böttcher, J.-N. Schmidt, J. Hertkorn, K. S. H. Ng, S. D. Graham, M. Guo, T. Langen, and T. Pfau, New states of matter with fine-tuned interactions: Quantum droplets and dipolar supersolids, Rep. Prog. Phys. **84**, 012403 (2021).

[8] I. Ferrier-Barbut, H. Kadau, M. Schmitt, M. Wenzel, and T. Pfau, Observation of Quantum Droplets in a Strongly Dipolar Bose Gas, Phys. Rev. Lett. **116**, 215301 (2016).

[9] M. Schmitt, M. Wenzel, F. Böttcher, I. Ferrier-Barbut, and T. Pfau, Self-bound droplets of a dilute magnetic quantum liquid, Nature (London) **539**, 259 (2016).

[10] L. Chomaz, S. Baier, D. Petter, M. J. Mark, F. Wächtler, L. Santos, and F. Ferlaino, Quantum-Fluctuation-Driven Crossover from a Dilute Bose-Einstein Condensate to a Macro-droplet in a Dipolar Quantum Fluid, Phys. Rev. X **6**, 041039 (2016).

[11] C. Cabrera, L. Tanzi, J. Sanz, B. Naylor, P. Thomas, P. Cheiney, and L. Tarruell, Quantum liquid droplets in a mixture of Bose-Einstein condensates, Science **359**, 301 (2018).

[12] G. Semeghini, G. Ferioli, L. Masi, C. Mazzinghi, L. Wolswijk, F. Minardi, M. Modugno, G. Modugno, M. Inguscio, and M. Fattori, Self-Bound Quantum Droplets of Atomic Mixtures in Free Space, Phys. Rev. Lett. **120**, 235301 (2018).

[13] C. D' Errico, A. Burchianti, M. Prevedelli, L. Salasnich, F. Ancilotto, M. Modugno, F. Minardi, and C. Fort, Observation of quantum droplets in a heteronuclear bosonic mixture, Phys. Rev. Research **1**, 033155 (2019).

[14] J. Wang, H. Hu, and X.-J. Liu, Thermal destabilization of self-bound ultradilute quantum droplets, New J. Phys. **22**, 103044 (2020).

[15] J. Wang, X.-J. Liu, and H. Hu, Ultradilute self-bound quantum droplets in Bose-Bose mixtures at finite temperature, Chin. Phys. B **30**, 010306 (2021).

[16] D. S. Petrov, Quantum Mechanical Stabilization of a Collapsing Bose-Bose Mixture, Phys. Rev. Lett. **115**, 155302 (2015).

[17] F. Minardi, F. Ancilotto, A. Burchianti, C. D'Errico, C. Fort, and M. Modugno, Effective expression of the Lee-Huang-Yang energy functional for heteronuclear mixtures, Phys. Rev. A **100**, 063636 (2019).

[18] H. Hu and X.-J. Liu, Consistent Theory of Self-Bound Quantum Droplets with Bosonic Pairing, Phys. Rev. Lett. **125**, 195302 (2020).

[19] H. Hu, J. Wang, and X.-J. Liu, Microscopic pairing theory of a binary Bose mixture with inter-species attractions: Bosonic BEC-BCS crossover and ultradilute low-dimensional quantum droplets, Phys. Rev. A **102**, 043301 (2020).

[20] Q. Gu and L. Yin, Phonon stability and sound velocity of quantum droplets in a boson mixture, Phys. Rev. B **102**, 220503(R) (2020).

[21] P. Zin, M. Pylak, and M. Gajda, Revisiting a stability problem of two-component quantum droplets, Phys. Rev. A **103**, 013312 (2021).

[22] X. Cui and Y. Ma, Droplet under confinement: Competition and coexistence with a soliton bound state, Phys. Rev. Research **3**, L012027 (2021).

[23] A. Gammal, T. Frederico, L. Tomio, and P. Chomaz, Liquid-gas phase transition in Bose-Einstein condensates with time evolution, Phys. Rev. A **61**, 051602(R) (2000).

[24] A. Bulgac, Dilute Quantum Droplets, Phys. Rev. Lett. **89**, 050402 (2002).

[25] D. Blume, B. D. Esry, C. H. Greene, N. N. Klausen, and G. J. Hanna, Formation of Atomic Tritium Clusters and Bose-Einstein Condensates, Phys. Rev. Lett. **89**, 163402 (2002).

[26] B. Gao, Universal properties of Bose systems with van der Waals interaction, J. Phys. B **37**, L227 (2004).

[27] I. Bešlić, L. Vranješ Markić, and J. Boronat, Quantum Monte Carlo simulation of spin-polarized tritium, Phys. Rev. B **80**, 134506 (2009).

[28] We note that the role of the three-body interaction on a quantum droplet in Bose-Bose mixtures has been emphasized in the work of J. Pan, S. Yi, and T. Shi, Quantum phases of self-bound droplets of Bose-Bose mixtures, arXiv:2102.02361.

[29] W. Zwerger, Quantum-unbinding near a zero temperature liquid–gas transition, J. Stat. Mech. (2019) 103104.

[30] P. M. A. Mestrom, V. E. Colussi, T. Secker, G. P. Groeneveld, and S. J. J. M. F. Kokkelmans, van der Waals Universality near a Quantum Tricritical Point, Phys. Rev. Lett. **124**, 143401 (2020).

[31] S. Tan, Three-boson problem at low energy and implications for dilute Bose-Einstein condensates, Phys. Rev. A **78**, 013636 (2008).

[32] S. Zhu and S. Tan, Three-body scattering hypervolumes of particles with short-range interactions, arXiv:1710.04147.

[33] H. Hu and X.-J. Liu, Collective excitations of a spherical ultra-dilute quantum droplet, Phys. Rev. A **102**, 053303 (2020).

[34] A. Griffin, Conserving and gapless approximations for an in-homogeneous Bose gas at finite temperatures, Phys. Rev. B **53**, 9341 (1996).

[35] D. A. W. Hutchinson, E. Zaremba, and A. Griffin, Finite Temperature Excitations of a Trapped Bose Gas, Phys. Rev. Lett. **78**, 1842 (1997).

[36] H. Shi and A. Griffin, Finite-temperature excitations in a dilute Bose-condensed gas, Phys. Rep. **304**, 1 (1998).

[37] Y. Kora, M. Boninsegni, D. T. Son, and S. Zhang, Tuning the quantumness of simple Bose systems: A universal phase diagram, Proc. Natl. Acad. Sci. USA **117**, 27231 (2020).

[38] D. T. Son, M. Stephanov, and H. U. Yee, The phase diagram of ultra quantum liquids, J. Stat. Mech. (2021) 013105.

[39] L. M. Satarov, M. I. Gorenstein, A. Motornenko, V. Vovchenko, I. N. Mishustin, and H. Stoecker, Bose–Einstein condensation and liquid–gas phase transition in strongly interacting matter composed of a particles, J. Phys. G **44**, 125102 (2017).

[40] F. Böttcher, M. Wenzel, J.-N. Schmidt, M. Guo, T. Langen, I. Ferrier-Barbut, T. Pfau, R. Bombín, J. Sánchez-Baena, J. Boronat, and F. Mazzanti, Dilute dipolar quantum droplets beyond the extended Gross-Pitaevskii equation, Phys. Rev. Research **1**, 033088 (2019).

[41] H. Hu and X.-J. Liu, Thermodynamics of a trapped Bose-Fermi mixture, Phys. Rev. A **68**, 023608 (2003).

[42] S. Giorgini, L. P. Pitaevskii, and S. Stringari, Condensate fraction and critical temperature of a trapped interacting Bose gas, Phys. Rev. A **54**, R4633(R) (1996).

[43] M. Barranco, R. Guardiola, S. Hernández, R. Mayol, J. Navarro, and M. Pi, Helium Nanodroplets: An overview, J. Low Temp. Phys. **142**, 1 (2006).

[44] D. Baillie, R. M. Wilson, and P. B. Blakie, Collective Excitations of Self-Bound Droplets of a Dipolar Quantum Fluid, Phys. Rev. Lett. **119**, 255302 (2017).

[45] X.-J. Liu, H. Hu, A. Minguzzi, and M. P. Tosi, Collective oscillations of a confined Bose gas at finite temperature in the random-phase approximation, Phys. Rev. A **69**, 043605 (2004).

[46] J. Wang, Hyperspherical approach to quantal three-body theory, Ph.D. thesis, University of Colorado Boulder, 2012.

[47] S. D. Hogan, A. W. Wiederkehr, H. Schmutz, and F. Merkt, Magnetic Trapping of Hydrogen after Multistage Zeeman Deceleration, Phys. Rev. Lett. **101**, 143001 (2008).

[48] A. W. Wiederkehr, S. D. Hogan, B. Lambillotte, M. Andrist, H. Schmutz, J. Agner, Y. Salathé, and F. Merkt, Trapping deuterium atoms, Phys. Rev. A **81**, 021402(R) (2010).

[49] B. M. Clark, Magnetic trapping of atomic tritium for neutrino mass measurement, B.S. thesis, California Institute of Technology, 2014.

[50] X.-J. Liu, H. Hu, and P. D. Drummond, Mean-field thermodynamics of a spin-polarized spherically trapped Fermi gas at unitarity, Phys. Rev. A **75**, 023614 (2007).